Ou *et al. Journal of NeuroEngineering and Rehabilitation* (2024) 21:196
https://doi.org/10.1186/s12984-024-01497-5

Journal of NeuroEngineering and Rehabilitation

RESEARCH **Open Access**

Detecting muscle fatigue among community-dwelling senior adults with shape features of the probability density function of sEMG

Jiarui Ou[1,2,3,4], Na Li[1,2,3], Haoru He[1,2,3], Jiayuan He[1,2,3], Le Zhang[4*] and Ning Jiang[1,2,3*]

Abstract

Background Physical exercise is an important method for both the physical and mental health of the senior population. However, excessive exertion can lead to increased risks of falls, severe injuries, and diminished quality of life. Therefore, simple and effective methods for fatigue monitoring during exercise are highly desirable, particularly in community settings. The purpose of this study was to explore the possibility of real-time detection of exercise-induced fatigue using surface Electromyogram (sEMG) features, including the kurtosis and skewness of the Probability Density Function (PDF) in the community settings to solve the issues of low sensitivity and high computational complexity of commonly used sEMG features.

Methods sEMG signals from six forearm muscles were recorded during hand grip tasks at 20% maximal voluntary contraction (MVC) task-to-failure contractions from 30 healthy community-dwelling elders at their respective community centers. PDF shape features of the sEMG, namely kurtosis and skewness, were computed from 25 s of non-fatigue stable phase and 25 s of fatigue data for comparison. Statistical tests were conducted to compare and test for the significance of these features. We further proposed a novel fatigue indicator, Temporal-Mean-Kurtosis (TMK) of channel-averaged kurtosis, to detect fatigue with relatively low computational complexity and adequate sensitivity in community settings. ANOVA and post-hoc analyses were performed to examine the performance of TMK.

Results Statistically significant differences were found between the non-fatigue period and the fatigue period for both kurtosis and skewness, with increasing values when approaching fatigue. TMK was shown to be sensitive in detecting fatigue with respect to time with lower computational complexity than the Sample Entropy.

Conclusion This study investigated PDF shape features of sEMG signals during a handgrip exercise to identify muscle fatigue in older adults in community experiments. Results revealed significant changes in kurtosis upon fatigue, indicating that PDF shape features were suitable convenient detectors of muscle fatigue in community experiments. The proposed indicator, TMK, showed potential sensitivity in tracking muscle fatigue over time in community-based

*Correspondence:
Le Zhang
zhangle06@scu.edu.cn
Ning Jiang
jiangning21@wchscu.cn
Full list of author information is available at the end of the article

settings with limited computational complexity, highlighting the promise of sEMG's PDF features in detecting muscle fatigue among the elderly.

Keywords Muscle fatigue, Surface electromyogram, Probability density function, Kurtosis, Higher-order statistics

Introduction

The global aging population presents multifaceted challenges to healthcare systems, particularly concerning age-related health issues such as musculoskeletal injuries [1–3], which present the foremost and pressing strain on the societies' healthcare infrastructure [3, 4]. It has been established that older adults need to perform physical exercises to maintain good physical and mental health [5–7]. However, it is essential to balance the amount and intensity of exercise to prevent exercise-induced injuries, which can lead to a decline in overall health and quality of life. Therefore, real-time detection of muscle fatigue during exercise is critical, especially in community settings where most seniors engage in physical activity.

Recent research proposed a novel approach: the assessment of perceived fatigability, which refers to the perception of effort or strain during a standardized physical activity [8, 9]. This concept has recently emerged as a valuable tool for identifying older adults who are at risk of experiencing greater-than-expected functional decline. Different constructs of fatigability can be measured using different standardized scales and questionnaires. For instance, state fatigability is usually measured using the Borg scale, while trait fatigability is measured through the Pittsburgh Fatigability Scale (PFS) rating [8, 10].

While standardized measurements of different constructs of the perceived fatigability provide potential subjective indicators, there is also a need for quick and effective objective methods to detect exercise-induced fatigue using convenient wearable devices, particularly in community settings, so that both the cognitively perceived fatigue and objective muscle fatigue could be incorporated together to provide concrete detection and warning of true fatigue in simple community exercises. Specifically, exercise-induced fatigue is characterized by a sensation of exhaustion, reduced muscle strength, and impaired coordination [11]. This decline of force impacts the functional abilities of older adults. Hence, real-time detection of muscle fatigue in community settings is vital for developing effective interventions and exercise programs tailored to the needs of older adults.

One promising approach for non-invasive detection of muscle fatigue involves the utilization of Surface Electromyography (sEMG), which is a technique used to record electrical signals generated by muscle fibers during activation [12, 13]. Features extracted from sEMG can be effective in reflecting changes in muscle fibers [14–16]. Traditional sEMG analyses focus on time-domain and frequency-domain features, such as the root mean square (RMS), which reflect changes in the strength or amplitude of the signal [15]. However, these features may not be sensitive enough to capture the finer structural or statistical changes within the signal that relates to muscle fiber conduction velocity and motor unit (MU) synchronization, especially when performing low-intensity exercises in community settings [17].

To solve the effectiveness issue, recent studies have explored non-linear properties of sEMG, such as the Sample Entropy (SampEn) [18], to reflect non-stationarities of signals during fatigue. However, one drawback of such non-linear properties is the high computational complexity.

Recently, to improve efficiency, the probability density function (PDF) of sEMG was investigated to detect muscle fatigue and MU number variations among healthy adults or in simulations [14, 19]. Specifically, the shape of sEMG's PDF has shown promise in reflecting the progression of fatigue, with observed deviations from the Gaussian distribution as fatigue sets in [14]. Shape descriptors of the PDF typically do not suffer from high computational complexity. Thus, they may also be effective indicators for the quick detection of muscle fatigue among older adults in communities with relatively low computational complexity. To be more specific, the skewness and kurtosis of PDFs were commonly used simple indicators to capture deviations from the Gaussian distribution. When the distribution of a PDF changes, skewness and kurtosis are expected to change accordingly with significance [20], thus, these features may be sensitive and easy-to-compute indicators of muscle fatigue for community experiments involving senior adults, a situation that has limited computational resources but demands adequate sensitivities.

Hence, this study aims to investigate the effectiveness and efficiency of using PDF shape features, specifically kurtosis and skewness, of sEMG signals as quick indicators of muscle fatigue during simple handgrip exercises involving older adults. The use of kurtosis could potentially provide a more convenient, low-complexity, and community-friendly method for real-time detection of muscle fatigue, enabling safer exercise programs for older adults. We also compared these EMG PDF features to conventional linear and non-linear features in fatigue detection. Based on that, we further proposed a temporally sensitive indicator with a low computational complexity for near real-time muscle fatigue detection based on the kurtosis, namely the Temporal-Mean-Kurtosis (TMK).

Methods

Participants

In this study, we recruited community-dwelling older adults aged 60 years and above from different communities in Chengdu, southwest China, with diverse socioeconomic conditions. To ensure the representation of diverse educational backgrounds and socioeconomic contexts, targeted recruitment announcements for older adults were published in four distinct communities. Eligibility criteria for enrollment comprised the ability to walk independently and a verified absence of severe muscular problems such as Parkinson's disease, sarcopenia, or stroke [21]. Conversely, exclusion criteria were as follows: [1] severe osteoarthritis; [2] unregulated diabetes; [3] unstable hypertension exceeding 150/90 mmHg; [4] documented cognitive impairments; [5] evidence of chronic organ failure within the last five years; and [6] any reported history of cancer. The participant must satisfy all the inclusion criteria and none of the exclusion criteria simultaneously to take part in the experiment. The requirement that the participant has to be able to walk without any walking aids is one of the inclusion criteria to ensure that the participant has adequate exercise ability and does not suffer from severe injuries or muscular diseases like sarcopenia, according to the Asian Working Group for Sarcopenia in 2019 Standards [22]. In this way, we can ensure that participants who finished the experiment were healthy and reliable senior adults (that they can at least maintain adequate exercise ability and feel muscle fatigue subjectively without large risks of injury). Following these criteria, a final cohort of 34 participants (16 men and 18 women) successfully completed all experimental protocols. The age of these 34 participants was 71.7 ± 6.2 years old. All participants were granted their informed written consent following a thorough explanation of the study procedures and attendant risks. This research adhered strictly to the tenets outlined in the Declaration of Helsinki and received ethical approval from the Institutional Review Board of the West China Hospital of Sichuan University under the reference number WCHSCU_2023_317.

Experimental protocol

Before the formal fatigue test, the forearm skin of each participant was gently shaved and then sanitized with an alcohol pad in order to establish optimal conditions for the recording of sEMG signals. On the participant's upper limb, six pairs of Ag/AgCl electrodes (Kendall H124SG, CardinalHealth Inc., Dublin, Ohio, USA) were affixed to the muscle bellies of the brachioradialis (BRD), flexor carpi radialis (FCR), flexor digitorum superficialis (FDS), flexor carpi ulnaris (FCU), extensor carpi ulnaris (ECU), and extensor digitorum (ED), as shown in Fig. 1(A). The exact placement of electrode pairs referred to the guidance according to the Atlas of Muscle Innervation Zone and Chap. 17 of Cram's Introduction to Surface Electromyography [23, 24]. Specifically, we first determine the anatomical landmark frames (ALF) of each targeted muscle and then place the electrodes upon optimal electrode sites with respect to the muscle anatomy according to guidelines stated in Cram's Introduction to Surface Electromyography (for FCR, FDS, FCU, and ED) [24] and Atlas of Muscle Innervation Zone (for BRD and ECU) [23]. The recording of signals was facilitated by a wireless system (Ultium EMG, Noraxon Inc., Scottsdale, USA) at a sampling rate of 2000 Hz and a gain setting of 1000. An example of recorded signals is exhibited in Fig. 1(C).

During the experiment session, the participants were seated naturally on a chair. They were then asked to place their arms naturally at the sides with the grip dynamometer held in the right hand, facing a computer screen to receive visual feedback. The main reasons for choosing this position instead of raising the elbow at 90°, as usual, are: [1] The Xiangshan handheld grip dynamometer (EH101 Grip Dynamometer, Xiangshan Inc., China) we were using is a small and convenient dynamometer that measures grip forces by pulling up a handle, so it measures more precisely when pulling vertically instead of pulling with the elbow twisted at 90° with the arms at sides. Indeed, this position we used in the experiment was the recommended position by the device manufacturer according to the operation manual, and [2] senior adults found it hard to maintain their elbow at 90° while performing handgrip tasks, especially when measuring MVCs continuously. The experimental protocol comprised two distinct parts, as presented in Fig. 1(B) and Fig. 1(C).

In part one, the participants were instructed to position their arms naturally at the sides and perform MVC trails by gripping a handheld dynamometer. The maximum grip force that the participant could sustain steadily for three to five seconds was recorded. Each participant repeated three MVC contractions with sufficient intertrial resting intervals. The average force value obtained from three trials was designated as the MVC reference force value for the participant.

Next, in part two, after a short familiarization period, participants perform a hand grip exercise at a force level equivalent to 20% of their MVC reference force until task failure. Specifically, after the participant's oral report of perceived fatigue, we then started to check the force reader on the grip dynamometer. If the force output was confirmed to be declined with the participant having difficulty maintaining the required force level, we considered the participant to be encountering fatigue for targeted muscles. Then, the participant was asked to try their best to maintain the grip force for an extra 25 s.

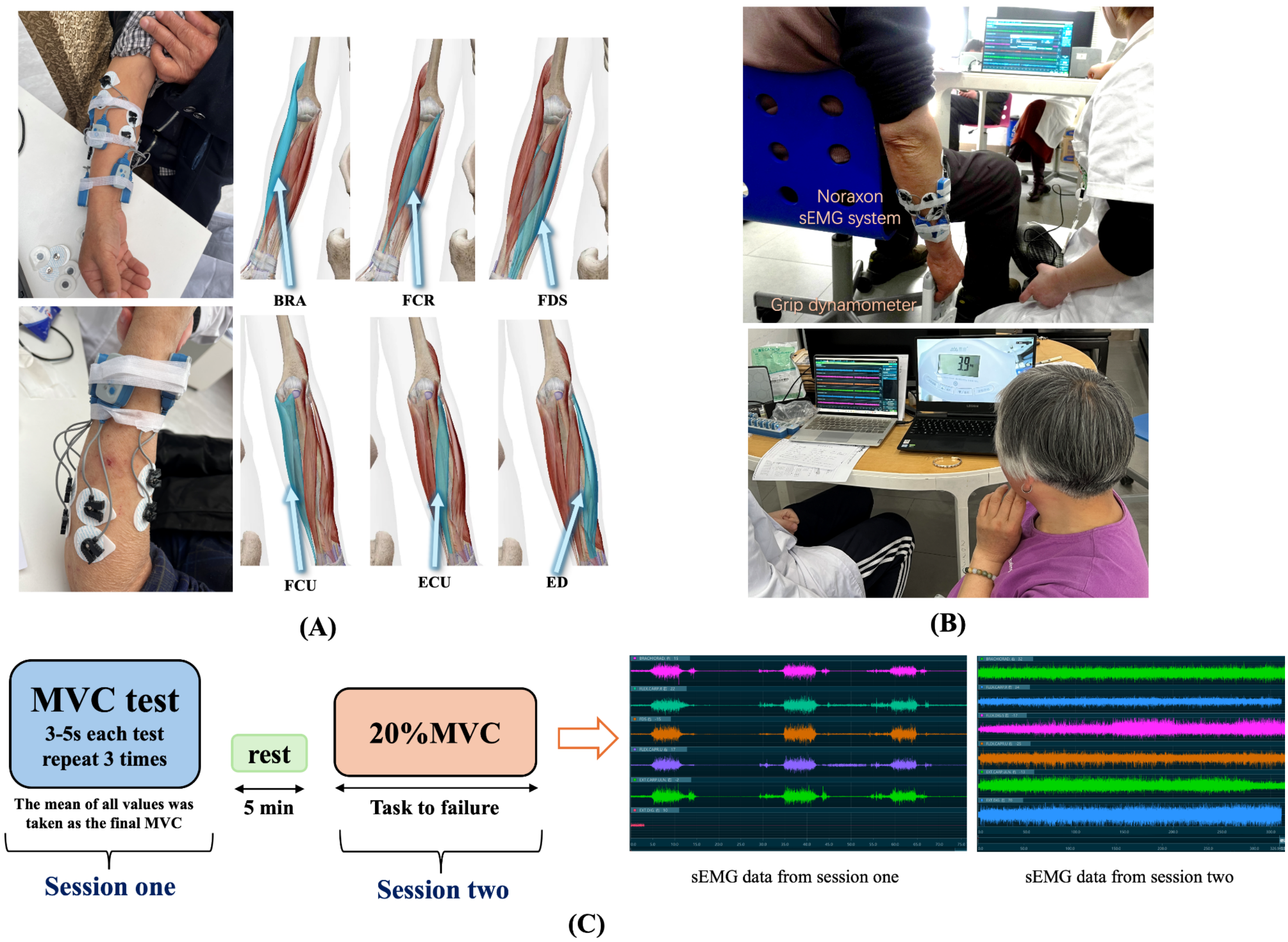

Fig. 1 The experimental protocol. (**A**). Illustration of the placement of six pairs of electrodes. (**B**). Photo of how the hand-grip fatigue experiments were conducted in communities. (**C**). Experimental procedure and the recorded sEMG signals from the two sessions

The sEMG data recorded during this period was considered fatigue data. The target force level was visually presented on the computer screen to guide the participants throughout the session. Typically, the entire experimental procedure did not exceed 15 min, a length well-tolerated by older adults and suitable for effective screening in community settings or at home.

Data processing

Data preprocessing

An sEMG expert inspected the acquired data to determine if there were abnormal channels with excessive noise or other artifacts to be addressed. Then, sEMG signals that met the standard without obvious problems were digitally filtered by notch filters of integral multiples of 50 Hz followed by a bandpass third-order Butterworth filter between 10 Hz and 500 Hz. In the end, data from four participants were excluded due to the absence of fatigue or problems in signal recording, and data from 30 participants were retained.

Feature extraction

The average duration of the recorded data is 337 s, with a standard deviation of approximately 80 s. The total duration did not affect the analysis methods too much because we selected the middle stable 25 s in the non-fatigue stage and the 25 s at the end of processed data, which is considered fatigue. So that the statistical tests can be carried out with as much power as possible with less variability in the temporal dimension. The sample size used for the statistical tests is determined by 20 windows of sEMG data for each phase (group) * 30 populations, resulting in a total number of 600 samples per group.

Specifically, to extract skewness and kurtosis from sEMG's PDF, we selected equal-length data from the non-fatigue and 25-second fatigue periods to perform statistical analysis. Specifically, five-second window segments with a one-second step size were applied to the pre-processed sEMG data. Then, 20 windows in the middle of the stable non-fatigue stage (typically between 50 s and 100 s on the timeline) and 20 windows at the end of the fatigue stage were extracted for group-wise statistical comparison tests.

For the calculation of kurtosis and skewness, after data preprocessing, empirical PDFs of the stable stage data and the fatigue stage data for each participant were estimated using the *KernelDensity* function in the *scikit-learn* package in Python. Then, sample kurtosis and sample skewness were computed according to Eqs. (1) and (2), respectively:

$$kurtosis = \left[\frac{n\,(n+1)}{(n-1)\,(n-2)\,(n-3)}\sum_{i=1}^{n}\left(\frac{X_i-\overline{X}}{S}\right)^4\right] - \frac{3(n-1)^2}{(n-2)\,(n-3)} \tag{1}$$

$$skewness = \frac{n}{(n-1)\,(n-2)}\sum_{i=1}^{n}\left(\frac{X_i-\overline{X}}{S}\right)^3 \tag{2}$$

where n is the total number of sampling points used to estimate the PDF (1000 in this study), X_i represents the *i*-th PDF value, $\bar{X}$ indicates the sample average of PDF values, and S is the sample standard deviation of all PDF values.

In addition to the above PDF shape features, for comparison purposes, root mean square (RMS) was also extracted according to Eq. (3) as a representation of time-domain features:

$$RMS = \sqrt{\frac{1}{m}\sum_{j=1}^{m}Y_i^2} \tag{3}$$

where m is the total number of time points, Y_i represents the *i*-th amplitude value.

Additionally, we calculated the change of the mean power frequency (MPF) to observe the actual onset of fatigue throughout the isometric contraction [15]. It is believed that MPF is a more reliable indicator of muscle fatigue in isometric contractions than time-domain features such as the RMS [15]. To confirm changes in MPF, we first determined and recorded the baseline MPF value for each participant through sEMG signals from the respective MVC trials. Then, the MPF values of the sEMG data from the non-fatigue and the fatigue protocol were calculated and normalized with respect to the baseline value for each participant. Following widely applied criteria in fatigue literature [15, 25], if a participant's MPF values from the fatigue protocol never decreased from the baseline, the participant possibly did not experience real muscle fatigue [14, 15, 25]. To extract MPF, a Fast Fourier Transform (FFT) with five-second non-overlapping temporal windows was first applied on non-segmented sEMG signals to obtain a discrete series of frequency spectrum amplitude, and then the power spectral density (PSD) was calculated using the square of frequency spectrum amplitude. Lastly, MPF was computed as the mean of all PSD [26].

Besides the above features from the time-domain, frequency-domain, and PDF, several other non-linear features were shown as effective in fatigue detections in recent studies, including the sample entropy (SampEn) and the Fractal Dimension [18, 27]. These non-linear features typically do not require stationarity assumptions of the signal [28] and are potentially effective in detecting underlying changing patterns of the sEMG considering muscle fatigue [17]. However, though effective, the computational complexity of non-linear features is typically high, making it difficult in community real-time detection experiments. Hence, we also took the SampEn as an example to compare the statistical significance and the computational complexity with PDF features for fast detection of fatigue in senior adults.

Outlier detections

After the initial feature extraction, outlier values were removed based on the following procedure. First, for non-fatigue data, outliers were excluded according to Grubbs' test since the PDF during non-fatigue periods still follows the Gaussian distribution [29]. For each of the feature values, it is considered as an outlier if it deviates more than $G_{\alpha,\,n}$ standard deviations apart from the mean, where $G_{\alpha,\,n}$ represents the numerical Grubbs' threshold [30], determined by the significance level $\alpha = 0.05$ and feature sample size. In the current study, the $G_{\alpha,\,n}$ values were set to 2.64 according to Grubbs' threshold Table (30). On the other hand, for fatigue stages, Grubb's rule cannot be applied because the fatigue EMG's PDF is no longer Gaussian by assumption [29, 31]. Hence, we utilized the interquartile range (IQR) method, which does not assume prior distributions of the sample, for outlier detections [31]. Specifically, an observation from the fatigue data was considered a potential outlier if it fell below (Q1–2 * IQR) or above (Q3+2 * IQR), where Q1 represents the first quartile and Q3 represents the third quartile. Lastly, a potential outlier was considered to be a true outlier and excluded for further analysis if it occurred less than twice among the previous and next two windows.

Statistical analysis of PDF shape features of sEMG in discriminating muscle fatigue

To conduct proper statistical tests for comparisons between the non-fatigue stage and the fatigue data for all features, since one of the key assumptions of the current study was unequal variances and deviations from the Gaussian distribution for data from the fatigue EMG, the Levene's test [32] for unequal variances ($p<0.01$) and

Shapiro-Wilk test [33] for Gaussianity ($p<0.05$) were first performed to confirm this assumption. As such, parametric tests were not applicable [34]. Hence, the non-parametric Mann-Whitney U test [34] was performed to test if statistically significant differences were presented between the 25 s of the non-fatigue data and the 25 s of fatigue data for each of the extracted features (kurtosis, skewness, RMS, MPF, and SampEn) for each sEMG channel. The significance and effectiveness of each feature were then compared to each other within each channel. Additionally, the mean-difference effect sizes (ES) and the corresponding 95% confidence intervals (CI) of the ES for each test statistic were calculated along with p-values.

Since multiple hypothesis tests were done on the same indicator across different channels to control the false discovery rate (FDR), the the Benjamini & Hochberg method [35] was applied to each family of test statistics, as it's the preferable approach for controlling Type-I errors in multiple testing because it not only reduces false positives, but also minimizes false negatives [36]. All statistical tests were performed at a significance level of 0.05.

Statistical analysis of temporal-mean-kurtosis as an indicator for muscle fatigue in community experiments

To better monitor and detect exercise-induced fatigue during community experiments with sufficient low complexity, a sensitive real-time indicator of fatigue based on the sEMG data was needed. Hence, we proposed to calculate a moving average version of the kurtosis of sEMG's PDF throughout the contraction experiments, namely the Temporal-Mean-Kurtosis (TMK), as a quantitative assessment for entering muscle fatigue. First, kurtosis was calculated using the same methodology as the previous section and then averaged over all six channels. Next, a non-overlapping 25-second sliding window was applied to the channel-averaged kurtosis curve. Lastly, the area under the kurtosis curve (indicated as the red line in Fig. 2) was calculated for each window as the TMK.

ANOVA statistical test was then used to examine differences among temporal levels. In the current study, each adjacent 25-second window is considered as one level in the ANOVA test. Moreover, to perform pairwise comparison among temporal levels and to determine which specific level differences were statistically significant after an overall significant difference, the Tukey's Honestly Significant Difference (HSD) test was utilized as a post-hoc analysis following ANOVA [37].

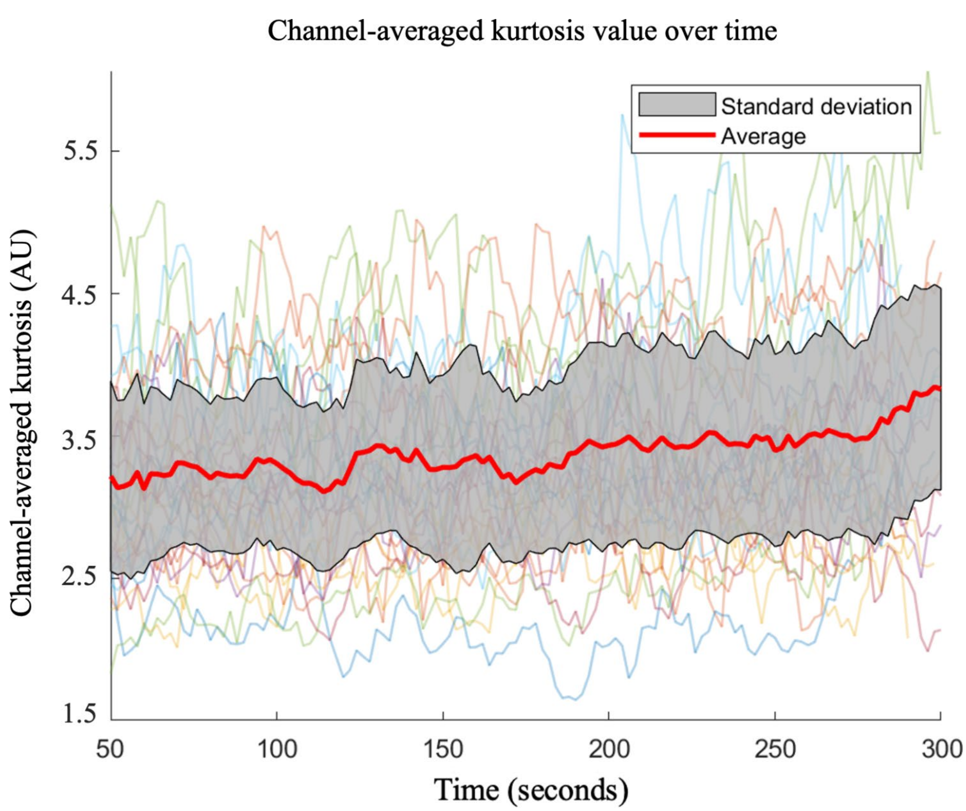

Fig. 2 Channel-averaged PDF kurtosis trend over time. The x-axis represents time in seconds. The y-axis represents the average PDF kurtosis value of all six channels of sEMG. The red line indicates the average of all participants, while the shaded grey area indicates ± one standard deviation

Table 1 Summarization table of descriptive statistics of the results averaged over all six channels

	Kurtosis	Skewness	Normalized RMS	Normalized MPF	Sample Entropy
Non-fatigue	3.107* (±0.595)	1.311* (±0.127)	0.436 (±0.174)	0.970* (±0.077)	1.215* (±0.070)
Fatigue	3.667* (±0.664)	1.467* (±0.225)	0.464 (±0.132)	0.906* (±0.078)	1.135* (±0.078)

Descriptive results are presented in the format of medians (± 1 *IQR*). The * indicates features (averaged over all six channels) that are statistically significant ($p<0.05$) using the Mann-Whitney U test

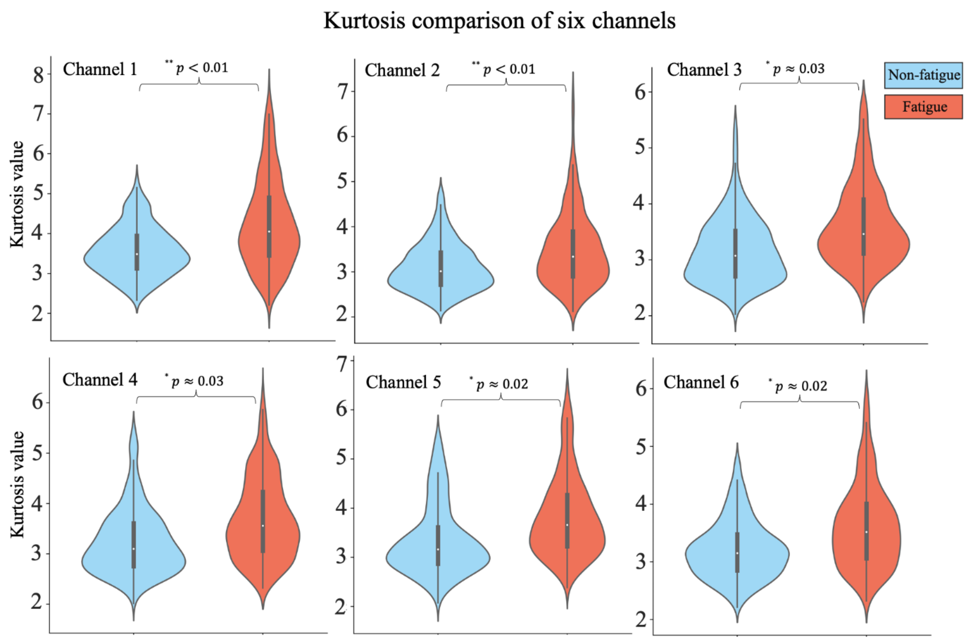

Fig. 3 Violin plots of within channel comparison of sEMG's PDF **kurtosis** between the non-fatigue versus fatigue stage

All computations were performed using Python version 3.11, *Scikit-learn* package version 1.4.1, *NumPy* package version 1.26.0, *SciPy* package version 1.12.0, *Pandas* package version 2.1.0, and *Seaborn* package version 0.13.2. All statistical tests were performed at a significance level of 0.05. All analyses were performed using R version 4.3.3 in RStudio software (Posit Co., United States).

Results

Statistical results of sEMG's PDF shape features in discriminating muscle fatigue

Descriptive statistics of the indicators

Descriptive statistics of all features were summarized in Table 1. As shown below, the kurtosis exhibited a significant increase when encountering fatigue, indicating a deviation from the Gaussian distribution of the sEMG's PDF. MPF was shown to be decreased as expected, but the extent of change is not as significant as the kurtosis.

Furthermore, referring to Sect. 2.4, using the Mann-Whitney U-test for all six channels, the resultant violin plots of kurtosis and skewness in distinguishing muscle fatigue are shown in Figs. 3 and 4, respectively. Here, Fig. 3 presents the differences in kurtosis distributions between the non-fatigue stage and the fatigue stage. All channels exhibited statistically significant differences in average kurtosis at the significance level of 0.05. Channels one and two presented the most obvious differences with the *p*-value smaller than 0.01. From the violin plot, it was also obvious that the kurtosis had higher values and larger ranges in general during fatigue compared to non-fatigue periods. This result showed that the kurtosis of PDF of sEMG was potentially a sensitive detector of muscle fatigue with our experimental protocol in elders, as it tended to increase when approaching fatigue, reflecting that the PDF was deviating from the Gaussian distribution with more extreme values in the sample.

Figure 4 shows the violin plots of differences in skewness distributions between the non-fatigue and the fatigue stage. Channel one, two, and six again obtained the most significant differences, with the *p*-value smaller than 0.02. Similar to kurtosis, skewness also tended to increase with fatigue, implying that the PDF was deviating from Gaussian with some right skews. But when compared to the extent to which kurtosis increased, skewness did not exhibit a much larger range and more extreme values as kurtosis showed. Combining together, the results showed that these two PDF shape features, especially the kurtosis, were sensitive in detecting exercise-induced fatigue in older adults. As well, the observed

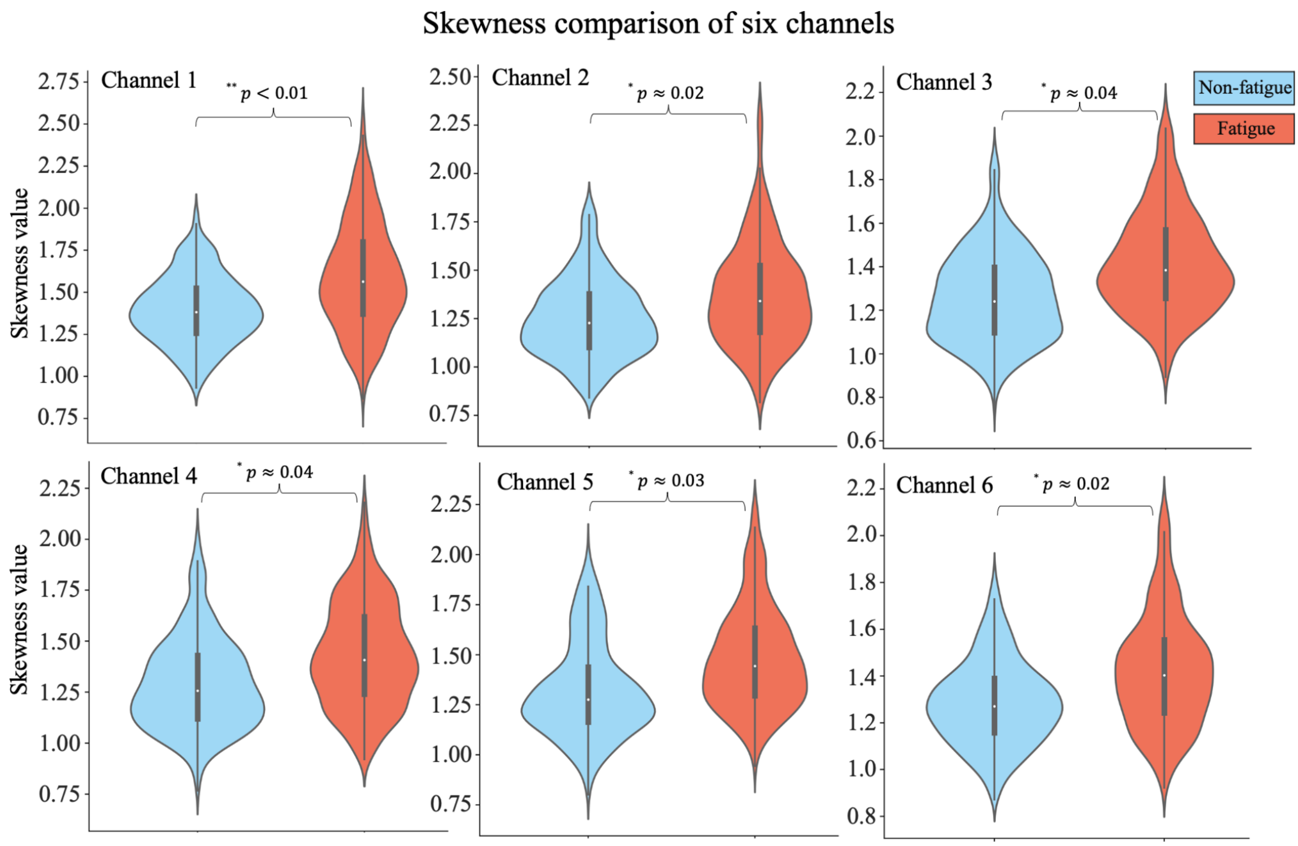

Fig. 4 Violin plots of within channel comparison of sEMG's PDF **skewness** between the non-fatigue versus fatigue stage

deviations from Gaussian distribution implied the presence of abnormal muscle activation or changes in MU recruitment/synchronization strategies during muscle fatigue.

Mann whitney U test results for group comparisons

Moreover, for comparison, differences in RMS, MPF, and SampEn between the non-fatigue and the fatigue period were also tested. As for RMS, the differences were not as obvious as PDF shape features in detecting muscle fatigue with our experimental protocol. Only channels two, three, and four showed statistically significant differences with a p-value smaller than 0.05 (but greater than 0.02 for all channels). The distinctions of RMS between the non-fatigue and fatigue stages were also not as clear and consistent as those two shape features of the sEMG PDF. This could potentially be due to difficulties of linear features in capturing subtle changes of signals' amplitude variations during low-effort exercises. MPF suffered from a similar situation. Though it was shown to be decreased, the significance was concerning. On the other hand, SampEn, as a representation of non-linear features, exhibited great significance between groups. The overall p-value comparison results are summarized in Table 2, along with the mean-difference effect sizes and corresponding 95% confidence intervals for the effect size.

FDR-adjusted p-value results

Last but not least, FDR-adjusted p-values are presented in Table 3. Results further showed that non-linear features generally exhibited statistical significance even after FDR adjustments, but RMS and MPF lost significance after controlling the FDR.

Performance of TMK as a temporal indicator for muscle fatigue

Figure 1 shows the development of averaged kurtosis over all six channels throughout the fatigue experiment from 50 s to 300 s. The x-axis represents the time, and the y-axis represents the averaged kurtosis values. The red line indicates the overall average of all 30 participants, while the shaded grey area indicates $\pm$ one standard deviation. It could be observed that the averaged kurtosis exhibited an increasing trend.

ANOVA results of the TMK

Furthermore, referring to Sect. 2.5, Fig. 5 depicts the TMK results of the averaged kurtosis curve (red line of Fig. 2) over the discretized 25-second temporal window.

Table 2 Summarization of *p*-value results

	Channel 1	Channel 2	Channel 3	Channel 4	Channel 5	Channel 6
Kurtosis	*p = 0.0095 ES = -0.746 CI = [-0.854, -0.639]	*p = 0.0078 ES = -0.826 CI = [-0.967, -0.686]	*p = 0.0292 ES = -0.458 CI = [-0.543, -0.374]	*p = 0.0335 ES = -0.401 CI = [-0.475, -0.328]	*p = 0.0201 ES = -0.465 CI = [-0.559, -0.370]	*p = 0.0235 ES = -0.465 CI = [-0.762, -0.168]
Skewness	*p = 0.0098 ES = -0.201 CI = [-0.231, -0.172]	*p = 0.0141 ES = -0.161 CI = [-0.213, -0.108]	*p = 0.0393 ES = -0.153 CI = [-0.179, -0.127]	*p = 0.0446 ES = -0.143 CI = [-0.203, -0.083]	*p = 0.0296 ES = -0.137 CI = [-0.164, -0.101]	*p = 0.0283 ES = -0.123 CI = [-0.146, -0.0998]
RMS	p = 0.0648 ES = -0.198 CI = [-0.280, -0.116]	*p = 0.0428 ES = -0.525 CI = [-1.048, -0.073]	p = 0.0503 ES = -0.339 CI = [-0.574, -0.104]	*p = 0.0435 ES = -0.369 CI = [-0.662, -0.077]	p = 0.0627 ES = -0.338 CI = [-0.535, -0.114]	p = 0.125 ES = -0.070 CI = [-0.290, -0.151]
MPF	p = 0.0704 ES = 0.026 CI = [0.010, 0.0504]	p = 0.0723 ES = 0.021 CI = [0.001, 0.041]	*p = 0.0402 ES = 0.052 CI = [-0.012, 0.116]	*p = 0.0340 ES = 0.092 CI = [0.0314, 0.153]	*p = 0.0420 ES = 0.032 CI = [-0.015, 0.0792]	p = 0.116 ES = 0.012 CI = [-0.011, 0.035]
Sample Entropy	*p = 0.0028 ES = 0.119 CI = [0.107, 0.131]	*p = 0.0129 ES = 0.095 CI = [0.079, 0.110]	*p = 0.0177 ES = 0.093 CI = [0.079, 0.107]	*p = 0.0367 ES = 0.041 CI = [0.030, 0.052]	*p = 0.0204 ES = 0.053 CI = [0.042, -0.065]	*p = 0.0084 ES = 0.077 CI = [0.062, 0.091]

*p represents p-value that is smaller than the significance level, i.e., 0.05, and thus exhibits statistically significant differences. ES = effect sizes. CI = confidence intervals for effect sizes.

Table 3 FDR adjusted *p*-value results

	Channel 1	Channel 2	Channel 3	Channel 4	Channel 5	Channel 6
Kurtosis	*p = 0.0285	*p = 0.0285	*p = 0.0335	*p = 0.0335	*p = 0.0335	*p = 0.0335
Skewness	*p = 0.0285	*p = 0.0285	*p = 0.0335	*p = 0.0335	*p = 0.0335	*p = 0.0335
RMS	p = 0.0776	p = 0.0776	p = 0.0776	p = 0.0776	p = 0.0776	p = 0.1250
MPF	p = 0.0723	p = 0.0723	p = 0.0723	p = 0.0723	p = 0.0723	p = 0.0723
Sample Entropy	*p = 0.0168	*p = 0.0245	*p = 0.0245	*p = 0.0367	*p = 0.0245	*p = 0.0245

*p represents adjusted p-value that is smaller than the significance level, i.e., 0.05, and thus exhibits statistically significant differences after FDR corrections

As shown, TMK results further confirmed the increasing trend in the variations of channel averaged kurtosis when approaching muscle fatigue, with the values starting from 250 s being significantly larger than those before 125 s. Indeed, ANOVA analysis carried out a p-value of 0.0076, which is obviously less than the significance level of 0.05, indicating that statistically significant differences existed among different time levels.

Tukey's HSD post-hoc analysis results of TMK among different time levels

As shown by the bars in Fig. 5, Tukey's HSD post-hoc analysis further showed that TMK values of the first two temporal levels, i.e., 75 to 100 and 100 to 125 s, were significantly less than that of the last time level when experiencing fatigue, i.e., 275 s to 300 s. Among all time levels, 100 to 125 s exhibited the greatest differences compared to the fatigue data (275 to 300 s), with an obvious increasing trend in TMK values, showing that the averaged kurtosis was experiencing an uprising when approaching fatigue.

Discussion

PDF shape features for detecting muscle fatigue

Significance of statistical test results

The primary aim of this preliminary study was to examine the effectiveness of using PDF shape features of sEMG signals as sensitive and convenient fatigue detectors during hand grip exercises for older adults using sustained low-effort contractions (20% MVC) in community settings. Statistical results showed that kurtosis exhibited the most significant differences between the non-fatigue stable stage and the task failure stage, reflecting a significant deviation from the Gaussian distribution, which potentially relates to MU activities regarding fatigue and aging [14, 16, 38–41]. In addition, ANOVA and post-hoc results showed that TMK is sensitive in detecting exercise-induced fatigue in community experiments.

The results together implied that, with the progression of muscle fatigue, the irregularity and complexity of muscle activity also varied. These results were consistent with some previous studies in PDF shape features used to detect various kinds of fatigue and further cross-validated that the PDF of sEMG signals tend to have higher peaks than Gaussian distribution when entering the fatigue stage [14, 16, 39, 41], even for older adults. In contrast, RMS had less significance in capturing subtle structural changes in sEMG caused by exercise-induced fatigue in low contraction levels among older adults. This is because linear features mainly detect variations in amplitudes or frequency spectrums, which do not change as significantly as the statistical properties of sEMG, especially during fatigue in low contraction levels. Also, it is hard for linear features to provide many insights into the

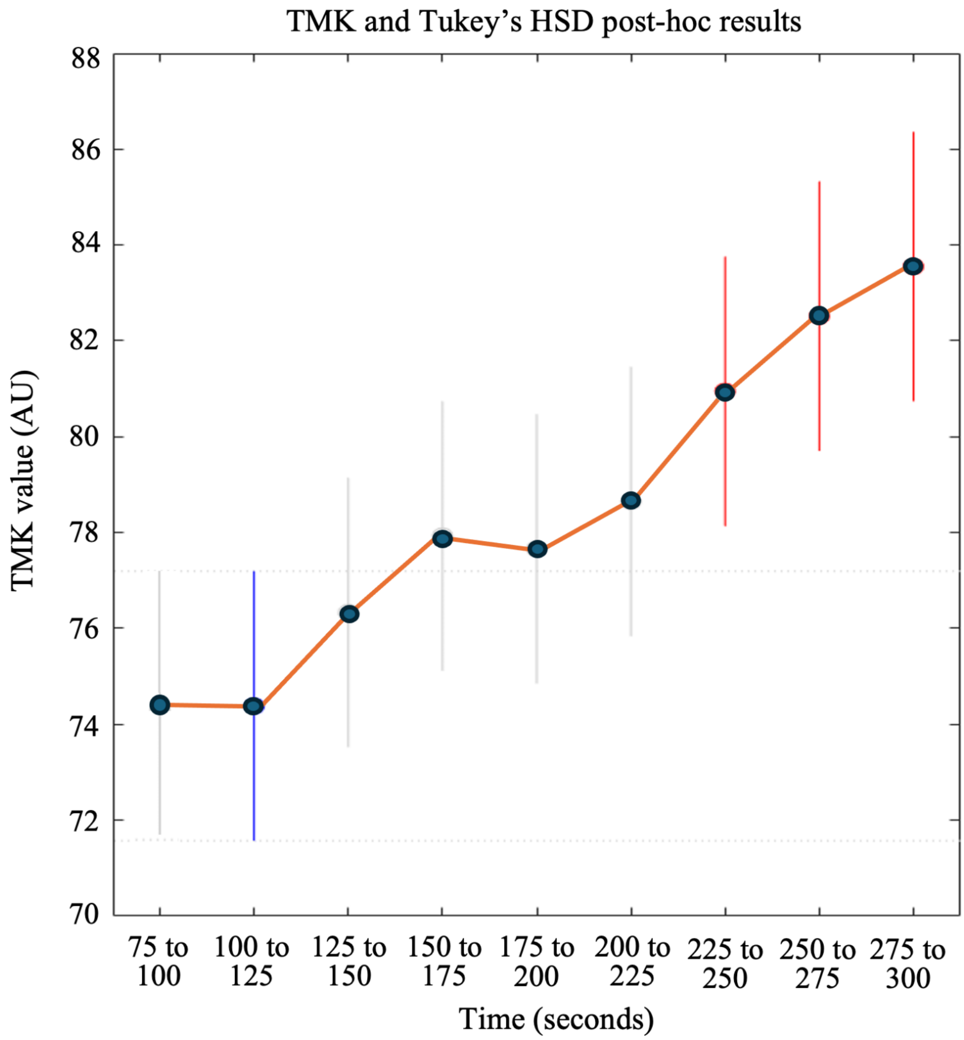

Fig. 5 TMK of channel-averaged kurtosis of every 25 s and Tukey's test results. The x-axis represents time in seconds. The y-axis represents the TMK values. Dots represent the TMK of that 25 s time period. Bars represent comparison intervals from the Tukey's test. Values outside the bar are considered significantly different. As shown, TMK from 100 to 125 s (blue bar) exhibited the most significant differences compared to the value from 275 to 300 s (red bar)

mechanism behind muscle fatigue in elders, as they cannot reflect statistical or in-depth structural changes [17]. As a result, the increase of TMK over time revealed that the PDF of sEMG signals occurred to have more extreme values that departed from the Gaussian distribution, representing the presence of abnormal variations regarding fatigue-related and age-related MU firing behaviors [17, 39], discussed further in Sect. 4.2.

Comparisons of the computational complexity

To facilitate a near real-time detection approach, the computational complexity of estimating the indicators is crucial to consider.

As for our approach involving the kurtosis indicator, the calculation process for a signal of length N meanly involves:

1) The fourth central moment calculation, which has a complexity of $O(N)$;
2) Calculations of the standard deviation, which also results in a complexity of $O(N)$;
3) Carrying out the kurtosis using the fourth central moment and the standard deviation, which involves a constant-time operation, resulting in a complexity of $O(1)$.

Hence, the overall complexity of the calculation involving the kurtosis of a signal of length N is dominated by $O(N)$.

In comparison, the sample entropy method [18] has a significantly higher computational complexity. To calculate the sample entropy for a signal of length N with embedded dimension of m, we need to go through processes of:

1) Subsequence generation, which results a complexity of $O(N)$;
2) Distance calculation, which involves calculating the distance of each subsequence to all others, resulting in a total complexity of $O((N-m+1)*(N-m)*m)$;
3) Probability calculation, which involves in a complexity of $O(1)$;
4) Carrying out the sample entropy using the probability, which involves a constant-time operation, resulting in a complexity of $O(1)$.

Therefore, the overall complexity of calculating a sample entropy indicator of a signal of length N and embedded dimension m is dominated by $O((N-m+1)*(N-m)*m)$. When $N \gg m$, this can be further simplified to $O(N^2 m)$. Apparently, this is much higher than the computational complexity of $O(N)$ for the kurtosis indicator.

Potential real-world applications

The near real-time detection of muscle fatigue using PDF features of sEMG signals holds significant promise for practical applications in community settings. With the advent of wearable technology and wireless systems, the proposed method could be integrated into portable devices designed for older adults. Such devices could continuously monitor sEMG signals during exercise, analyze them using PDF features like the TMK, and alert users or caregivers when signs of fatigue are detected. For instance, a wearable sensor on the forearm could transmit sEMG data to a smartphone app, which would display TMK values in real-time. If the TMK value indicates fatigue, the app could advise taking a break or reducing exercise intensity. This approach would help prevent exercise-induced injuries and enable older adults to maintain safe exercise routines, thereby improving their health and quality of life. The method's simplicity and low computational complexity make it ideal for integration into community fitness programs and home exercise equipment, facilitating widespread adoption.

Interpretations, mechanisms, and implications

Mechanisms behind the neuromuscular junction system and motor units

Indeed, to better detect fatigue in community experiments and study the mechanisms behind muscle fatigue involving the neuron-muscular system, capturing the variations of MU synchronizations or recruitments is very crucial since MU is one of the fundamental grouping units that is responsible for the muscle's ability for accurate and refined motions [11]. A motor unit (MU) comprises a single motoneuron and the ensemble of muscle fibers it innervates. When a motion is initiated, the efferent neural drive activates the motoneuron, triggering the generation of a series of motor unit action potentials (MUAPs). These MUAPs are then conducted to the neuromuscular junction (NMJ) and subsequently transmitted to the muscle fibers, initiating muscle contraction [42, 43].

To thoroughly examine the complex interactions within this system and the resulting complexity of sEMG signals, non-linear methods are particularly advantageous. At both the probabilistic and information density levels, these methods can capture the intricate patterns and distributions of MUAPs, as well as any abnormal activities, through probabilistic or density representations at the micro level [17, 27, 44]. Some other studies further suggested that the uplifting in MU synchronization when approaching fatigue might serve as a method to compensate for motoneuron excitability and concentrated MU recruitment after exercise-induced fatigue [4,36]. The decreasing trend of the sample entropy observed in other research is also in line with the interpretation that MU synchronization is more concentrated during fatigue [12, 16, 27], potentially caused by different distributions of type I and type II MUs from non-fatigue to fatigue in older adults [14, 45, 46].

Regarding the results from this study and related interpretations, the increase in kurtosis and the changes in the skewness of the sEMG's PDF are indicative of more extreme values departing from the Gaussian distribution. This is likely related to abnormal variations in MU firing behaviors due to aging and fatigue. Specifically, the increase in kurtosis suggests a concentration of MU recruitment, which aligns with the observed increase in MU synchronization during fatigue mentioned above. The changes in skewness may indicate a shift in MU type distributions from non-fatigue to fatigue states in older adults [14].

The effects and potential interpretations of MU aging

In older adults, there is a reduction and increased variability in synaptic inputs that activate motor neurons, a decline in the number of motor units combined with an enlargement in their size, decreased stability of neuromuscular junctions, lower and more variable discharge rates of MUAPs [47]. Additionally, Aged MUs exhibit distinct type I and type II MU distributions, leading to more sophisticated patterns of muscle fatigue [14]. Statistically, these structural changes affect the trends in the shape and distance of PDFs derived from sEMG signals [14], which can be generalized to effectively study the changes in MU synchronization and recruitment during fatigue among older adults.

Generalization to regular Exercise monitoring

Speaking of generalization, the findings of this study can be generalized to the monitoring of muscle fatigue during exercises among senior adults who perform low-effort exercises regularly in communities. This subgroup of senior adults particularly demands simple and effective means to detect potential exercise-induced fatigue during their regular exercises to avoid severe injuries. The use of sEMG signal analysis, especially focusing on the shape features of the PDF, can provide a convenient and sensitive method for detecting the onset of fatigue using wireless systems. This is crucial for preventing the impact of functional abilities and reduction in quality of life for this subgroup of senior adults in community settings.

Limitations and future directions

Although the kurtosis and skewness of PDF of sEMG signals revealed significant differences between the non-fatigue and the fatigue stage in our community experiments, several limitations of this study should be addressed.

Firstly, the effectiveness of PDF shape features using higher order statistics only occurred and was tested with a sustained low contraction in our setup. The sensitivity of higher order statistics of PDF was still not clear for more complicated exercises that are close to daily sports, which involve excessively large areas of different muscles and underlying MUs [38, 48, 49]. For such activities, sEMG signals can vary drastically with high complexity, bringing further challenges in sensitively detecting fatigue of each muscle.

Additionally, for fast screening purposes and current limitations to our dynamometer devices, mechanical properties were not simultaneously performed with sEMG experiments [50]. Though time-consuming, actual power and mechanical properties using mechanomyography (MMG) can provide direct information about muscle force variations and potential insights into muscle activation properties [50]. Importantly, we can further conduct sensitivity comparison analyses involving PDF shape features compared to other traditional sEMG features by performing a correlation test between the actual power and such features [25]. Hence, in future studies, sensitive sEMG features combined with mechanical features are of great interest in detecting muscle fatigue through more complicated exercises among older adults in daily community settings.

Moreover, the participants of this study were recruited only in a specific city in China, lacking generalizations worldwide. Thus, larger datasets involving more comprehensive population inclusion are necessary for future experiments.

Lastly, besides limitations regarding objective measurements, the absence of directly measuring perceived fatigability for senior adults [8] instead of oral reports and sEMG features represents a gap that could be addressed in future experiments since the lack of fatigability measurements can introduce bias in perceived reports of fatigability. Although previous research indicated that fatigability can also be measured by quantifying declines in several aspects of muscular performance or declines in accuracy over time on continuous tasks [51], such as the ARV of sEMG in performance tasks [52], the Borg scale is more beneficial in providing a standardized and validated method for assessing the state fatigability. Plus, the PFS can help with standardized measurements of the trait fatigability, potentially enhancing the predictive power of the fatigability and sports performance assessment combined together.

A final note on future directions is regarding Machine Learning methods. From statistical analyses on non-linear indicators, useful features can then be beneficial in machine learning and deep learning algorithms to classify or even forecast muscle fatigue with high accuracy and sensitivity [38, 53]. But, for such models, datasets are extremely crucial in order for the machines to learn properly and effectively. Hence, augmenting the dataset is also an important future work to do.

Conclusion

This study has demonstrated the feasibility of using the kurtosis and skewness of the Probability Density Function (PDF) of sEMG signals to detect exercise-induced muscle fatigue in community-dwelling older adults. The findings show that the Temporal Mean Kurtosis (TMK) is a sensitive indicator of muscle fatigue, offering a practical and community-friendly method for fatigue monitoring during exercise. The results suggest that the use of PDF shape features can provide a simple yet effective approach to detecting muscle fatigue in near real-time, which is particularly relevant for community settings.

Looking ahead, the development of wireless systems that incorporate these PDF features could facilitate the broader implementation of fatigue monitoring tools in daily exercise routines. Such systems would enable older adults to engage in safe and effective physical activity, thereby reducing the risk of exercise-induced injuries and improving overall health and well-being. Considering the growing global aging population and the increasing demand for community-based exercise programs, the findings of this study highlight the importance of developing accessible and efficient methods for monitoring muscle fatigue to prevent falls and injuries among older adults, ultimately enhancing their quality of life and independence.

Abbreviations

sEMG	Surface Electromyogram
PDF	Probability density function

TMK	Temporal Mean Kurtosis
MVC	Maximal voluntary contraction
RMS	Root mean square
MPF	Mean power frequency
SampEn	Sample Entropy
MU	Motor unit
CV	Conduction velocity
PFS	Pittsburgh Fatigability Scale
ALF	Anatomical Landmark Frames
MPF	Mean power frequency
BRA	Brachioradialis
FCR	Flexor carpi radialis
FDS	Flexor digitorum superficialis
FCU	Flexor carpi ulnaris
ECU	Extensor carpi ulnaris
ED	Extensor digitorum
FFT	Fast Fourier Transform
PSD	Power spectral density
IQR	Interquartile range
ES	Effect size
CI	Confidence interval
ANOVA	Analysis of Variance
HSD	Tukey's Honestly Significant Difference test
NMJ	Neuromuscular junction
MUAPs	Motor units action potentials
MMG	Mechanomyography

Acknowledgements
The authors would like to thank the assistance of the community workers in our data collection.

Author contributions
J.O.: Conceptualization; Formal analysis; Investigation; Methodology; Visualization; Writing - original draft; Writing - review & editing. N.L.: Data curation; Investigation; Methodology. H.H.: Data curation. J.H.: Conceptualization; Resources; Supervision; Validation. L.Z.: Methodology; Resources; Funding acquisition; Supervision; Project administration. N.J.: Conceptualization; Funding acquisition; Methodology; Project administration; Resources; Supervision; Validation; Writing - review & editing.

Funding
This work was supported by the Key Research Project Grant from the National Clinical Research Center for Geriatrics (No. Z2023YY001), Chengdu Key R&D Support Program - Technological Innovation R&D Project (No. 2022-YF05-01904-SN), 1.3.5 Project for Disciplines of Excellence from West China Hospital (#ZYYC22001), National Natural Science Foundation of China (No. 62372316), National Science and Technology Major Project (Nos. 2021YFF1201200 and 2018ZX10201002, China), Sichuan Science and Technology Program (No. 2022YFS0048), and Chongqing Technology Innovation and Application Development Project (No. CSTB2022TIAD-KPX0067).

Data availability
Anonymized data are made available from the corresponding authors upon reasonable request.

Declarations

Ethics approval and consent to participate
The study was conducted by the declaration of Helsinki and approved by the ethics subcommittee of West China Hospital of Sichuan University (WCHSCU_2023_317).

Consent for publication
Not applicable.

Competing interests
The authors declare no competing interests.

Author details
[1]The National Clinical Research Center for Geriatrics, West China Hospital of Sichuan University, Chengdu, Sichuan 610041, China
[2]Medical Equipment Innovation Research Center, West China Hospital of Sichuan University, Chengdu, Sichuan 610041, China
[3]The Med-X Center for Manufacturing, Sichuan University, Chengdu, Sichuan 610041, China
[4]College of Computer Science, Sichuan University, Chengdu 610065, China

Received: 7 June 2024 / Accepted: 27 October 2024
Published online: 04 November 2024

References

1. Rudnicka E, Napierała P, Podfigurna A, Męczekalski B, Smolarczyk R, Grymowicz M. The World Health Organization (WHO) approach to healthy ageing. Maturitas. 2020;139.
2. Akimov AV, Gemueva KA, Semenova NK. The Seventh Population Census in the PRC: results and prospects of the Country's Demographic Development. Her Russ Acad Sci. 2021;91(6):724–35.
3. Li L, Du T, Hu Y. The Effect of Population Aging on Healthcare expenditure from a Healthcare demand perspective among different age groups: evidence from Beijing City in the People's Republic of China. Risk Manage Healthc Policy. 2020;13:1403–12.
4. Holloszy JO, Faulkner JA, Brooks SV, Zerba E. Muscle atrophy and weakness with aging: Contraction-Induced Injury as an underlying mechanism. Journals Gerontology: Ser A. 1995;50A(SpecialIssue):124–9.
5. Arabzadeh E, Karimi Nazar N, Gholami M, Roshani Koosha MS, Zargani M. The effect of eight weeks combined training with omega-3 supplementation on the levels of intercellular adhesion molecule-1 and vascular cell adhesion molecule-1 in older women. Clin Nutr ESPEN. 2024;61:151–7.
6. Ferreira LG, Krajnak J, Paludo AC, Gimunova M, Svobodová L, Stein AM. Effect of exercise detraining in cognitive functions of older adults: a systematic review. Arch Gerontol Geriatr. 2024;125:105485.
7. Cadore EL, Izquierdo M. Enhancing health outcomes in institutionalized older adults: the critical role of combined exercise and nutritional interventions. J Nutr Health Aging. 2024;28(5):100267.
8. Simonsick EM, Glynn NW, Jerome GJ, Shardell M, Schrack JA, Ferrucci L. Fatigued, but not Frail: Perceived Fatigability as a marker of Impending decline in mobility-intact older adults. J Am Geriatr Soc. 2016;64(6):1287–92.
9. Glynn NW, Qiao Y. Measuring and understanding the health impact of greater fatigability in older adults: a call to action and opportunities. Fatigue: Biomed Health Behav. 2023;11(2–4):188–201.
10. Simonsick EM, Schrack JA, Santanasto AJ, Studenski SA, Ferrucci L, Glynn NW. Pittsburgh Fatigability Scale: one-page predictor of mobility decline in mobility-intact older adults. J Am Geriatr Soc. 2018;66(11):2092–6.
11. Gandevia SC. Spinal and supraspinal factors in human muscle fatigue. Physiol Rev. 2001;81(4):1725–89.
12. Cifrek M, Medved V, Tonković S, Ostojić S. Surface EMG based muscle fatigue evaluation in biomechanics. Clin Biomech Elsevier Ltd. 2009;24(4):327–40.
13. He J, Niu X, Zhao P, Lin C, Jiang N. From forearm to wrist: deep learning for Surface Electromyography-based gesture recognition. IEEE Trans Neural Syst Rehabil Eng. 2024;32:102–11.
14. Krishnan B, Zanelli S, Boudaoud S, Scapucciati L, McPhee J, Jiang N. Age-sensitive high density surface electromyogram indices for detecting muscle fatigue using core shape modelling. Biomed Signal Process Control. 2023;81:104446.
15. Sun J, Liu G, Sun Y, Lin K, Zhou Z, Cai J. Application of Surface Electromyography in Exercise fatigue: a review. Front Syst Neurosci. 2022;16:893275.
16. Marco G, Alberto B, Taian V. Surface EMG and muscle fatigue: multi-channel approaches to the study of myoelectric manifestations of muscle fatigue. Physiol Meas. 2017;38(5):R27–60.
17. Yang H-c, Wang D-m, Wang J, editors. Linear and Non-Linear Features of Surface EMG during Fatigue and Recovery Period. 2005 IEEE Engineering in Medicine and Biology 27th Annual Conference; 2005 17–18 Jan. 2006.
18. Wang S, Tang H, Wang B, Mo J. Analysis of fatigue in the biceps brachii by using rapid refined composite multiscale sample entropy. Biomed Signal Process Control. 2021;67:102510.
19. Zhao Y, Li D. A simulation study on the relation between muscle motor unit numbers and the non-Gaussianity/non-linearity levels of surface electromyography. Sci China Life Sci. 2012;55(11):958–67.
20. Kim HY. Statistical notes for clinical researchers: assessing normal distribution (2) using skewness and kurtosis. Restor Dent Endod. 2013;38(1):52–4.

21. Cruz-Jentoft AJ, Sayer AA, Sarcopenia. Lancet. 2019;393(10191):2636–46.
22. Chen LK, Woo J, Assantachai P, Auyeung TW, Chou MY, Iijima K, et al. Asian Working Group for Sarcopenia: 2019 Consensus Update on Sarcopenia diagnosis and treatment. J Am Med Dir Assoc. 2020;21(3):300–e72.
23. Barbero M, Merletti R, Rainoldi A, editors. Atlas of muscle innervation zones. Springer Milan; 2012.
24. Criswell E. Chapter 17: Electrode Placements. Cram's Introduction to Surface Electromyography. Second Edition ed: Jones & Bartlett Learning; 2010.
25. Wang L, Wang Y, Ma A, Ma G, Ye Y, Li R, et al. A comparative study of EMG indices in muscle fatigue evaluation based on Grey Relational Analysis during All-Out Cycling Exercise. Biomed Res Int. 2018;2018:9341215.
26. LIU J, ZOU R, ZHANG D, XU X, Xiufang H. Research and Development Trend of feature extraction methods of Surface Electromyogrphic signals. Progress Biomedical Eng. 2015;36(3):5.
27. Rampichini S, Vieira TM, Castiglioni P, Merati G. Complexity Analysis of Surface Electromyography for assessing the Myoelectric Manifestation of Muscle Fatigue: a review. Entropy [Internet]. 2020; 22(5).
28. Talebinejad M, Chan ADC, Miri A. A lempel–Ziv complexity measure for muscle fatigue estimation. J Electromyogr Kinesiol. 2011;21(2):236–41.
29. Grubbs FE. Procedures for detecting outlying observations in samples. Technometrics. 1969;11(1):1–21.
30. Grubbs FE, Beck G. Extension of sample sizes and percentage points for significance tests of outlying observations. Technometrics. 1972;14(4):847–54.
31. Dallah D, Sulieman H, editors. Outlier detection using the range distribution. Advances in Mathematical modeling and Scientific Computing; 2024 2024//; Cham: Springer International Publishing.
32. Gastwirth JL, Gel YR, Miao WW. The impact of Levene's test of Equality of variances on statistical theory and practice. Stat Sci. 2009;24(3):343–60.
33. Lanzante JR. Testing for differences between two distributions in the presence of serial correlation using the Kolmogorov-Smirnov and Kuiper's tests. Int J Climatol. 2021;41(14):6314–23.
34. Wilcox RR. Chapter 5 - comparing two groups. In: Wilcox RR, editor. Introduction to robust estimation and hypothesis testing. Fifth Edition): Academic. 2022;153–251.
35. Benjamini Y, Hochberg Y. Controlling the false Discovery rate: a practical and powerful Approach to multiple testing. J Roy Stat Soc: Ser B (Methodol). 2018;57(1):289–300.
36. Jafari M, Ansari-Pour N, Why. When and how to adjust your *P* values? Cell J. 2019;20(4):604–7.
37. Agbangba CE, Sacla Aide E, Honfo H, Glèlè Kakai R. On the use of post-hoc tests in environmental and biological sciences: a critical review. Heliyon. 2024;10(3):e25131.
38. Ayachi FS, Boudaoud S, Marque C. Evaluation of muscle force classification using shape analysis of the sEMG probability density function: a simulation study. Med Biol Eng Comput. 2014;52(8):673–84.
39. Holtermann A, Grönlund C, Karlsson JS, Roeleveld K. Motor unit synchronization during fatigue: described with a novel sEMG method based on large motor unit samples. J Electromyogr Kinesiol. 2009;19(2):232–41.
40. Furui A, Tsuji T, editors. Muscle Fatigue Analysis by Using a Scale Mixture-based Stochastic Model of Surface EMG Signals. 2019 41st Annual International Conference of the IEEE Engineering in Medicine and Biology Society (EMBC); 2019 23–27 July 2019.
41. McManus L, Hu X, Rymer WZ, Suresh NL, Lowery MM. Muscle fatigue increases beta-band coherence between the firing times of simultaneously active motor units in the first dorsal interosseous muscle. J Neurophysiol. 2016;115(6):2830–9.
42. Datta AK, Stephens JA. Synchronization of motor unit activity during voluntary contraction in man. J Physiol. 1990;422(1):397–419.
43. Luca CJD, Roy AM, Erim Z. Synchronization of motor-unit firings in several human muscles. J Neurophysiol. 1993;70(5):2010–23.
44. Burhan N, Kasno M, Ghazali R, editors. Feature extraction of surface electromyography (sEMG) and signal processing technique in wavelet transform: A review. 2016 IEEE International Conference on Automatic Control and Intelligent Systems (I2CACIS); 2016 22–22 Oct. 2016.
45. Ling SM, Conwit RA, Ferrucci L, Metter EJ. Age-Associated Changes in Motor Unit Physiology: observations from the Baltimore Longitudinal Study of Aging. Arch Phys Med Rehabil. 2009;90(7):1237–40.
46. Piasecki M, Ireland A, Jones DA, McPhee JS. Age-dependent motor unit remodelling in human limb muscles. Biogerontology. 2016;17(3):485–96.
47. Hunter SK, Pereira HM, Keenan KG. The aging neuromuscular system and motor performance. J Appl Physiol. 2016;121(4):982–95.
48. Mijnarends DM, Meijers JMM, Halfens RJG, ter Borg S, Luiking YC, Verlaan S, et al. Validity and reliability of tools to measure muscle Mass, Strength, and physical performance in Community-Dwelling Older people: a systematic review. J Am Med Dir Assoc. 2013;14(3):170–8.
49. Al Harrach M, Boudaoud S, Carriou V, Laforet J, Letocart AJ, Grosset J-F, et al. Investigation of the HD-sEMG probability density function shapes with varying muscle force using data fusion and shape descriptors. Comput Biol Med. 2017;89:44–58.
50. Tian SL, Liu Y, Li L, Fu WJ, Peng CH. Mechanomyography is more sensitive than EMG in detecting age-related Sarcopenia. J Biomech. 2010;43(3):551–6.
51. Kluger BM, Krupp LB, Enoka RM. Fatigue and fatigability in neurologic illnesses: proposal for a unified taxonomy. Neurology. 2013;80(4):409–16.
52. Beretta-Piccoli M, Cescon C, Barbero M, Villiger M, Clijsen R, Kool J, et al. Upper and lower limb performance fatigability in people with multiple sclerosis investigated through surface electromyography: a pilot study. Physiol Meas. 2020;41(2):025002.
53. Jiang Y, Malliaras P, Chen B, Kulić D. Real-time forecasting of exercise-induced fatigue from wearable sensors. Comput Biol Med. 2022;148:105905.

Publisher's note